Observations of Circumstellar Disks and Jets

Claire J. Chandler & John S. Richer

Department of Physics, University of Cambridge, Cavendish Laboratory, Madingley Road, Cambridge CB3 0HE, United Kingdom

Abstract. Measurements of the physical properties of disks around young, low-mass stars have shown that many resemble our current picture for the early solar system. Inner holes appear after a few $\times 10^6$ yr, perhaps caused by the formation of large bodies such as planets, and high-resolution imaging of young systems is beginning to constrain models of disk structure. There is considerable evidence that energetic mass loss is directly connected to accretion during star formation. Multiple knots and bowshocks in optical jets suggest accretion is far from steady, and there is clear evidence that jet directions wander on timescales of $\sim 10^4$ yr. An underlying driving jet is able to explain many features of the molecular outflows detected from deeply embedded protostars, but cannot account for the smooth conical structures observed for some older sources. A wide-angle wind may therefore also be needed.

1. Introduction

The formation of disks around young stars is a natural consequence of star formation from the gravitational collapse of molecular gas with non-zero angular momentum (Bodenheimer 1995). Approximately 50% of optically-visible, solar-mass, pre-main sequence (T Tauri) stars are surrounded by disks (e.g., Beckwith et al. 1990), and a motivating force in many studies of these disks has been the possibility that they represent proto-planetary systems. Measurements of their physical properties may therefore provide a direct connection between theories of star formation and the product with which we are most familiar: the Sun and the solar system. It is during the earliest phases of disk evolution, when the solid material resides in relatively small dust particles, that these systems are most easily detected. Much of the current work has therefore concentrated on determining the masses, temperature and density distributions, and kinematics of disks associated with stars $\lesssim 10^6$ yr old.

The recent dramatic increase in our understanding of circumstellar disks has been the result of the increase in spatial resolution available with the Hubble Space Telescope and with millimetre-wave interferometers. High-resolution imaging has also helped immensely in establishing the role of collimated jets in star formation, and these jets may be very closely connected to disk accretion via magneto-hydrodynamic disk winds (e.g., Pudritz, this volume). Indeed, the ubiquity of energetic mass loss during the very early stages of star formation suggests that jets, outflows, and winds are essential for making stars, perhaps representing the mechanism which removes the angular momentum from disk material, enabling matter to accrete onto the central protostar.

This review describes the techniques used to study disks around low-mass ($\lesssim$ 3 $M_\odot$) stars, summarises their observational properties, and discusses the connection between mass loss and accretion in star formation.

2. Circumstellar disks

2.1. Observations of embedded protostars and T Tauri stars

Most of the dust and molecular gas in a disk around a young solar mass star has a temperature in the range 10 to 100 K, and emits radiation at far-infrared and submillimetre wavelengths. Integrated spectral energy distributions are often well fitted by models of disk spectra, particularly for those T Tauri stars which are relatively isolated from emission from the surrounding molecular cloud. In the nearby star-forming regions of Taurus and ρ Ophiuchus a disk 100 AU in diameter subtends only $0.7''$ on the sky. Nevertheless, single-dish surveys for millimetre dust emission ($\theta_{\rm beam} \sim$ 10–$30''$) provided some of the first evidence that the dust had to be distributed in a flattened structure, this geometry being needed to reconcile the particle masses implied by the large millimetre fluxes with the lack of optical extinction to the central star (Beckwith et al. 1990). The median mass of T Tauri disks derived from the optically-thin millimetre dust emission is typically a few $\times$ 0.01 $M_\odot$ (Beckwith et al. 1990; André & Montmerle 1994; Osterloh & Beckwith 1995).

The high resolution provided by the HST and adaptive optics on ground-based optical and infrared telescopes has produced some of the most spectacular images of circumstellar disks, seen in absorption against the background illumination of the Orion nebula (McCaughrean & O'Dell 1996; McCaughrean et al. 1998), and through stellar photons scattering off dust particles in the disk surfaces (e.g., Smith & Terrile 1984; Burrows et al. 1996; Close et al. 1997). However, it is important to remember that even at the resolution provided by the HST, the extended optical and infrared emission originates not from disk material being viscously heated to several thousand degrees, but from photospheric emission scattered off the upper and lower surfaces of cool disk material. The presence of near-infrared emission in excess of that expected from the stellar photosphere can be used to infer the presence of warm dust in the disk within a few stellar radii, but *direct* imaging of the disk emission is best carried out at millimetre wavelengths where the size scales of the emission are well matched to the resolution and sensitivity available with current instruments.

Since the first direct measurements of disk sizes, made using submillimetre interferometry between the Caltech Submillimeter Observatory and the James Clerk Maxwell Telescope on Mauna Kea, Hawaii (Lay et al. 1994), the radii of a number of dust disks have now been determined (e.g., Lay et al. 1995; Dutrey et al. 1996; Kitamura et al. 1996). Typical radii of $\sim$ 50 to 100 AU are observed for T Tauri and protostellar disks, with major axes oriented perpendicular to optical or molecular hydrogen jets in most cases.

The evidence for disks in systems younger than optically-visible pre-main sequence stars is confused by the presence of extended envelopes of gas and dust around embedded protostars. The envelope causes extinction which obscures

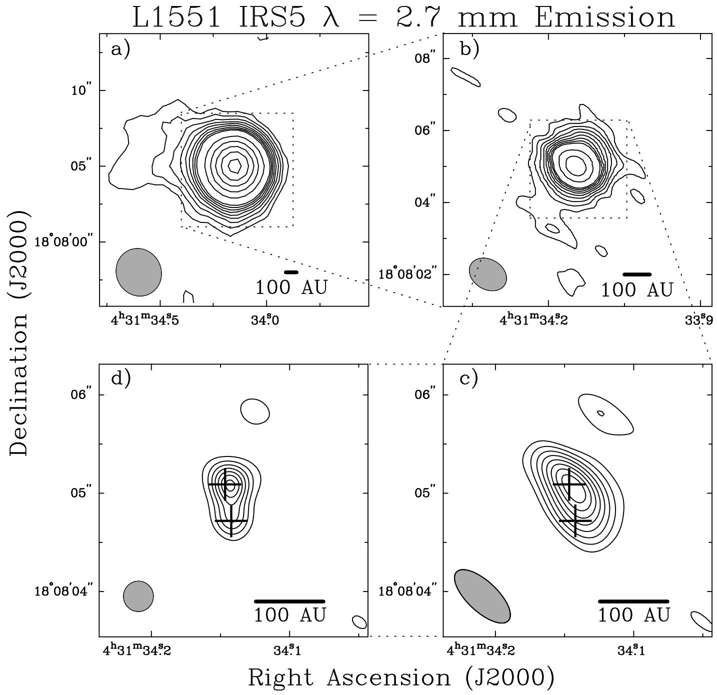

Figure 1. Maps of the $\lambda = 2.7$ mm dust continuum emission from L1551-IRS5 made using the BIMA millimetre array (Looney et al. 1997). (a) and (b) are images obtained by including all the spatial frequencies measured, tracing the extended envelope; (c) and (d) are images of only the high spatial frequency data, illustrating compact dust emission is associated with each component of a binary system.

the infrared emission from the disk, and adds an extended emission component in the millimetre which must be disentangled from the disk, requiring the use of interferometers as spatial filters. An excellent example of how millimetre interferometry can isolate an embedded protostar from its envelope is shown in Figure 1, which illustrates the emission from L1551-IRS5 imaged using the BIMA array at Hat Creek, California (Looney et al. 1997). An image made using all the low spatial frequency data primarily traces the extended envelope; as the low spatial frequencies are removed and only the high frequencies are included, the images reveal a binary system, with each component of the binary surrounded by a compact dust disk. Approximately 25% of the $\lambda = 2.7$ mm flux from L1551-IRS5 originates in the two circumstellar disks. For even younger systems (ages $\lesssim 10^4$ yr) not detected at near- or mid-infrared wavelengths ('Class 0' protostars: André et al. 1993) only 10% of the millimetre emission may arise in a disk (e.g., Pudritz et al. 1996). Nevertheless, the disk masses obtained for deeply embedded protostars are approximately the same as those for pre-main sequence stars. It is therefore not clear that the disk growth predicted by a number of recent models (Stahler et al. 1994; Nakamoto & Nakagawa 1995; Saigo & Hanawa 1998) has yet been observed.

2.2. Persistence timescales and evolution

Once a pre-main sequence star becomes optically visible its age can be estimated from model isochrones, allowing trends in the presence of near-infrared excesses and millimetre emission as a function of stellar age to be examined. The compilation of millimetre survey data by Osterloh & Beckwith (1995) shows no correlation between the 1.3 mm flux, which traces the relatively cool material at large radii in the disks, and stellar age. However, measurements of disk emission in the near-infrared (Skrutskie et al. 1990), which traces the inner regions of disks, do indicate a deficit of emission possibly corresponding to the presence of holes in inner disks for stars older than $\sim 10^7$ yr. More recently, Dutkevitch (1995) has suggested that the holes may be appearing in stars as young as 10^6 yr. These results suggest that the inner regions of the disks are being cleared before the outer parts responsible for the millimetre emission; possible clearing mechanisms include the Poynting-Robertson effect, and the formation of large bodies such as planets in the disks (Backman & Paresce 1993). The disk structure at large radii can be affected by the close proximity of a stellar companion, however. Binary systems with separations between ~ 1 and 50–100 AU have significantly lower millimetre and submillimetre fluxes than single stars or wide binaries (Jensen et al. 1994, 1996; Osterloh & Beckwith 1995).

The evidence for disk dispersal obtained from dust spectra has recently been confirmed by direct images of somewhat older stars. These post-T Tauri objects are closer than the star forming complexes, providing increased linear resolution, but their disks are less massive and until now have been much harder to detect. The sensitive submillimetre camera SCUBA on the JCMT has recently imaged the long-wavelength dust emission from four main sequence stars, and mid-infrared cameras such as MIRLIN on the Keck can now provide images of the warm dust close to the central stars.

HR 4796A HR 4796A is a young A0 star with an age of $\sim 10^7$ yr. Strong mid- to far-infrared emission in excess of that expected from the stellar photosphere was detected by IRAS (Jura 1991), making it a very good candidate for imaging the disk emission as soon as sensitive mid-infrared cameras became available (Jayawardhana et al. 1998; Koerner et al. 1998). Figure 2 shows a composite image of the 12.5-μm emission, which primarily originates from the central star and the very inner regions of the disk, and the 20-μm emission, which traces more extended and cooler dust. The 20-μm data show that an inner hole is required, with a radius of ~ 55 AU, to explain the observed distribution.

Fomalhaut, Vega, β Pictoris, ϵ Eridani The cool dust disks around young main sequence stars have been imaged using SCUBA (Holland et al. 1998; Greaves et al. 1998), but the linear resolution of a single-dish submillimetre telescope limits the identification of holes in the disks to very nearby sources. Fomalhaut (spectral type A3V) is only 8 pc distant, and has an age of $\sim 2 \times 10^8$ yr. Its disk is almost edge-on, and shows clear evidence of an inner hole with a radius of ~ 30 AU (Figure 3). Vega (A0V) lies at a similar distance but is almost face-on, and may be somewhat older than Fomalhaut ($\sim 4 \times 10^8$ yr). Once the photospheric emission from the star is subtracted it too may have a hole in the inner regions of its circumstellar disk. β Pictoris (A5V) is associated with a

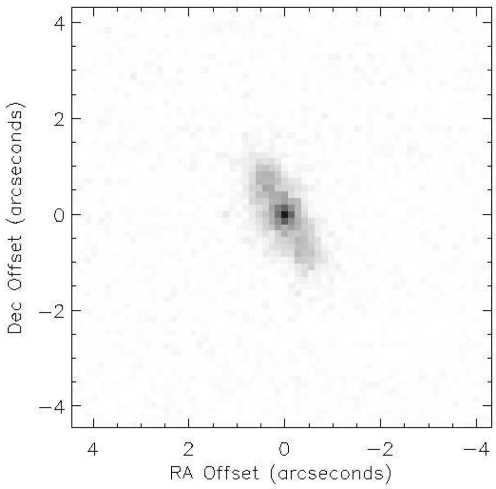

Figure 2. Image of the total 12.5 and 20-μm dust emission from HR 4796A, obtained using the MIRLIN mid-infrared camera on the Keck (Koerner et al. 1998). The emission traces an edge-on disk, with an inner hole ~ 55 AU in radius.

substantial dust disk, but its larger distance limits observation of its structure to measurements of warps and asymmetries in the distribution of scattered optical light (Kalas & Jewitt 1995; Burrows et al. 1995). The dust ring recently detected around the solar-mass star ϵ Eridani (K2V) may be even more similar to the young solar system (Greaves et al. 1998). Its proximity ($D = 3.2$pc) has enabled SCUBA to resolve a structure analogous to a young Kuiper belt. The typical dust masses of disks detected around young main-sequence stars is a few $\times$ $M_{\rm moon}$ ($\sim 10^{23}$ kg).

2.3. Comparison with α-disk models

Disks mediate accretion and angular momentum transport during star formation, so circumstellar disk structure is often analysed using the simplifying assumptions of steady α-disks (Shakura & Sunyaev 1973). It is unlikely that the α-prescription for the kinematic viscosity is appropriate for transport of angular momentum by MHD disk winds at small disk radii, however. Furthermore, the evidence for time-dependent accretion during FU Orionis outbursts (accretion rates $\dot{M}_{\rm acc}$ of $\sim 10^{-4}$ $M_\odot$ yr^{-1} compared with 10^{-7}–10^{-9} $M_\odot$ yr^{-1} commonly measured for quiescent T Tauri stars) may indicate that the accretion of most of the mass onto the central star is determined by disk instabilities (Livio, this volume) rather than viscosity. Nevertheless, the α-prescription may be reasonable if the low-level accretion, between outbursts and at large disk radii, is controlled by a mechanism such as the Balbus-Hawley instability (Hawley, this volume); ionization fractions $\gtrsim 10^{-13}$ couple the gas to the magnetic field sufficiently for this viscosity mechanism to operate (Gammie 1996).

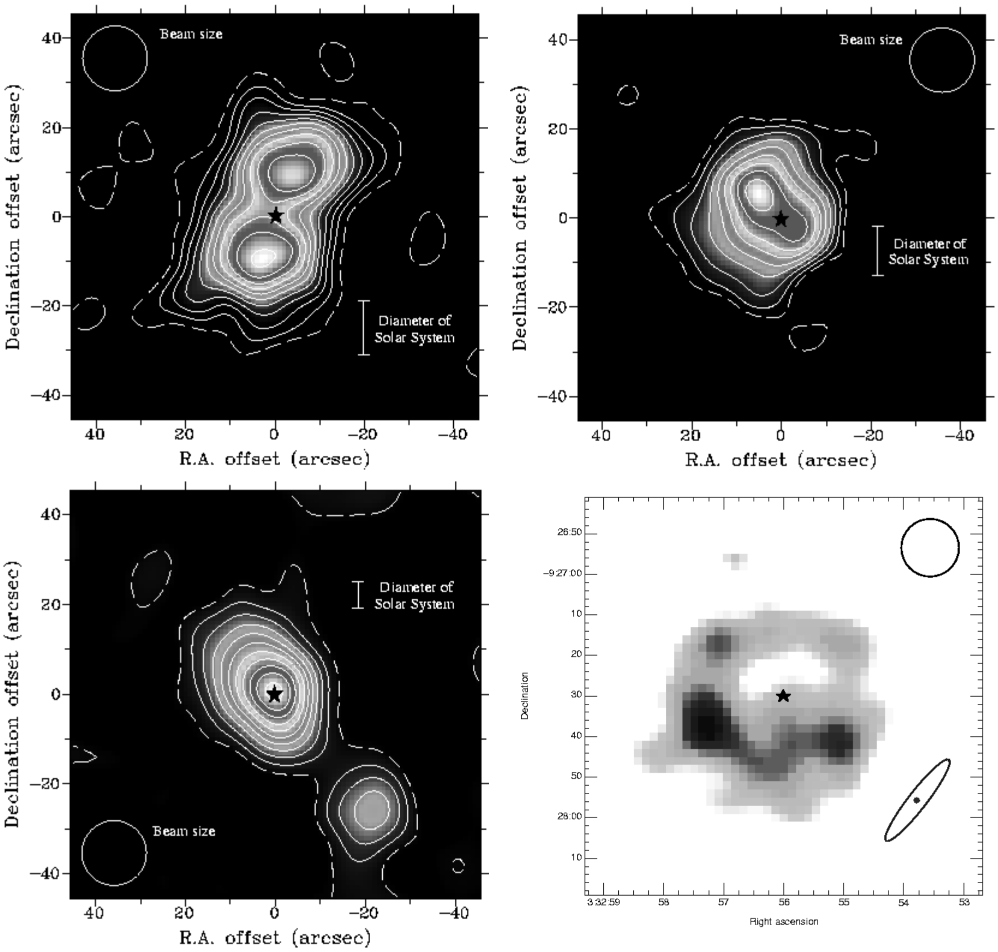

Figure 3. The 850-μm emission from cool dust disks around four main sequence stars, imaged using SCUBA on the JCMT (Holland et al. 1998; Greaves et al. 1998). A clear hole is detected for Fomalhaut (top left), and once the stellar emission from Vega (top right) has been subtracted it too shows a deficit of disk emission towards the star. β Pictoris (bottom left) is more distant and a hole cannot be resolved. ϵ Eridani (bottom right) is surrounded by a dust ring similar to a young Kuiper belt; the beam size is given in the top right of the panel, and the size of Pluto's orbit is bottom right.

The α-disk models are certainly attractive in that they make testable predictions. For a constant $\dot{M}_{\rm acc}$ the surface density is determined by the kinematic viscosity, which in the α-prescription gives a radial power law, typically $\Sigma \propto r^{-1}$. If the disk emission is optically thick and the gravitational energy is dissipated locally, the temperature profile is predicted to be $T \propto r^{-3/4}$ (Pringle 1981). This same value of $d\log T/d\log r = -3/4$ is also obtained for disks heated by absorbing and re-radiating energy from the central star (Adams & Shu 1986). Measurements of $d\log T/d\log r$ from optically-thick infrared T Tauri disk spectra show that very few objects have temperature profiles falling as steeply as the $r^{-3/4}$ expected for steady accretion disks or reprocessing disks; most have $T \propto r^{-0.5}$ (Beckwith et al. 1990; Henning et al. 1993; Osterloh & Beckwith 1995). A possible explanation is that these sources are surrounded by tenuous dust envelopes which absorb radiation from the star and disk, scattering and re-emitting photons which heat the disks at large radii (Natta 1993).

The surface density distribution can potentially provide very important constraints on the nature of the viscosity, but is somewhat harder to measure, because sub-arcsecond resolution is needed to image the direct disk emission. The sample of T Tauri stars observed by Dutrey et al. (1996) using the IRAM millimetre interferometer at Plateau de Bure, France, comprises one of the few data sets which has sufficient resolution to measure apparent angular sizes of the dust disks for a significant number of sources. By comparing the sizes with a power-law temperature and surface density model, Dutrey et al. conclude that $\Sigma \propto r^{-1}$ (see also Mundy et al. 1996; Lay et al. 1997). A similar result has been obtained through modelling the scattered optical light in HST images of HH30 (Burrows et al. 1996). This profile is consistent with α-disks having $d\log T/d\log r \lesssim -0.5$.

The disk kinematics can be determined in regions where the continuum emission is optically thin, i.e., the outer regions ($r \gtrsim 50$ AU) traced by molecular rotational transitions at millimetre wavelengths, or from the very inner regions of the disk where the dust is destroyed. Figure 4 illustrates Keplerian rotation in a ring of gas and dust surrounding the binary system GG Tau in Taurus (Dutrey et al. 1994). The central hole in the circumbinary disk has been caused by tidal interactions between the disk and the binary system, and the kinematics are consistent with rotation in the ring about a total central mass of 1.2 $M_\odot$. The inner edge of the ring has also been detected in scattered near-infrared light through imaging using adaptive optics, and infrared excesses suggest that each component of the binary system is also surrounded by a small circumstellar disk (Roddier et al. 1996).

At radii of a few $\times\ R_*$ emission lines such as the rotation-vibration bands of CO at 2.3 μm have excitation requirements well matched to the conditions expected in the inner regions of accretion disks. Near-infrared CO bandhead emission has been detected towards several young stars now, in some cases with velocities of ~ 200 km s^{-1} (Carr & Tokunaga 1992; Carr et al. 1993; Chandler et al. 1993). The bandhead profiles are very well modelled by the characteristic double-peaked profile of a disk, illustrating Keplerian rotation on scales of a few stellar radii (Chandler et al. 1995; Najita et al. 1996).

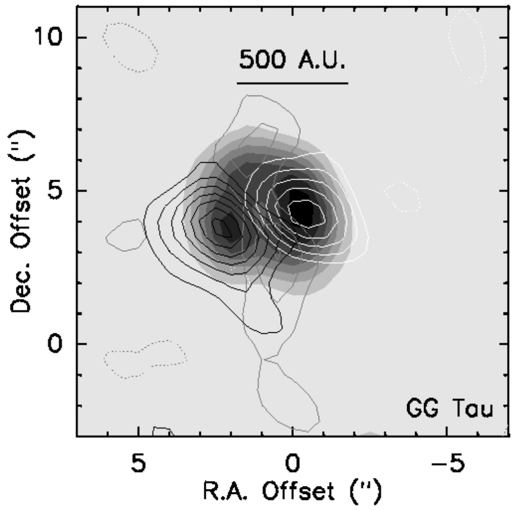

Figure 4. Composite image of the $\lambda = 2.7$ mm dust continuum emission (greyscale) and the ^{13}CO J=1–0 emission from the circumbinary ring around GG Tau (Dutrey et al. 1994). The molecular emission at velocities blueshifted and redshifted by 1.3 km s^{-1} relative to systemic are given in black and white contours respectively, while the systemic emission is in grey.

3. Optical jets and molecular outflows

3.1. Observations of jets and flows

From the start of accretion during the embedded phase to their appearance as optically-visible T Tauri stars, protostars are associated with energetic mass loss. Highly-collimated optical jets are found emanating from stars with low extinction (e.g., Ray et al. 1996; Reipurth & Heathcote 1997), and velocities of several 100 km s^{-1} suggest the jets must originate deep within the gravitational potential well of the central star. Bowshocks and internal working surfaces in the jets are typically traced by the emission from Hα, [SII], [OI], and [NII]. For the very youngest and deeply embedded protostars, mass loss is evident only because the surrounding molecular gas is swept up to velocities of 10s to 100s of km s^{-1} by an invisible wind or jet from the central source (Bachiller 1996; Padman et al. 1997). In some cases near-infrared H_2 emission traces the recent passage of shocks where the wind impacts the ambient material (e.g., McCaughrean et al. 1994; Eislöffel 1997).

Early low-resolution observations of molecular outflows from young protostars presented a picture of relatively poorly-collimated structures (Lada 1985), which purely from morphological considerations questioned whether optically-visible jets were in any way related to the mass loss observed in deeply embedded sources. Further problems arose from comparisons of the momentum supply rates derived for both phenomena, which for optical jets fell short of that

Figure 5. HST image of the [SII] and Hα emission from HH34 (courtesy of J. Hester). Knots and internal working surfaces are evident within the highly-collimated jet, which originally was thought to terminate in the Hα-bright bowshock 0.2 pc from the embedded protostar. The flow is now known to extend over several parsecs.

required to power the molecular flows by at least two orders of magnitude. As long as the jet was assumed to be fully ionized and the optical emission therefore traced all the jet material, typical jet densities of $n_{\rm j} \sim 10$ cm^{-3} were derived (Mundt et al. 1987). The dynamical timescales obtained from the ratio of the jet or flow length to the observed velocity were also highly discrepant, with $\tau_{\rm dyn}$(opt) $\sim 10^2$–10^3 yr and $\tau_{\rm dyn}$(mol) $\sim 10^4$–10^5 yr.

With the discovery of the highly-collimated and jet-like molecular flows (e.g., Richer et al. 1992; Cernicharo & Reipurth 1996) and a re-analysis of the optical jet data (e.g., Hartigan et al. 1994) these discrepancies are beginning to diminish. The optical jets are now believed 95–99% neutral, with $n_{\rm j} \sim 10^3$ cm^{-3}. The recent large-scale imaging of optical jets also shows that the jets can extend several parsecs from the driving source (e.g., Bally et al. 1996; Devine et al. 1997; Reipurth et al. 1997), much further than previously thought, and estimates of dynamical ages of optical flows are coming into closer agreement with molecular outflows (Eislöffel & Mundt 1997). The flow associated with HH34 is an excellent example, initially believed to comprise only the jet directly associated with the central infrared source, and the bowshock at HH34 (Figure 5). Eislöffel & Mundt (1997) and Devine et al. (1997) now find successive bowshocks and patches of nebulosity in Hα and [SII] emission extending many arcminutes from the driving source. These features also trace a symmetric "S"-shape suggesting that the direction of the jet has been changing in time, and that the jet must be ballistic.

That jets drive molecular outflows has become extremely clear in cases such as L1448 and HH211 (Figure 6). The HH211 flow was initially discovered through its strong, shocked H_2 emission, and the protostar itself is not detected even at 2 μm. High-resolution interferometer images of the millimetre line emission from SiO illustrates that dense gas is directly associated with the jet; at several locations the SiO emission coincides with H_2 shocks (Chandler & Richer 1997). High-velocity CO emission is also observed along the central axis

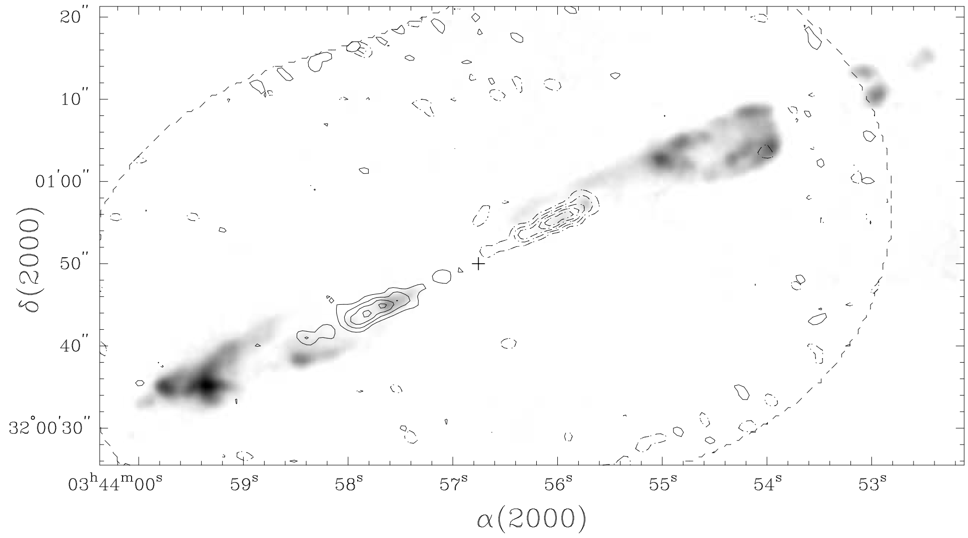

Figure 6. Grey-scale of the shocked molecular hydrogen emission from HH211 (McCaughrean et al. 1994) beneath contours of the blue-shifted (solid lines) and redshifted (dot-dashed lines) SiO J=1–0 emission from the driving jet (Chandler & Richer 1997). The position of the embedded protostar is marked by a cross.

of the flow, with slower-moving material outlining a sheath around the near-infrared H_2 emission (Guilloteau et al. 1997). Such measurements are essential for establishing how ambient material is entrained and accelerated by jets, an understanding of which is needed if the properties of the underlying jet are to be determined.

3.2. Accretion–mass loss connection

Although there are well-developed theoretical ideas linking mass loss in jets with disk accretion, the connection is difficult to demonstrate observationally. The extreme jet velocities detected imply that even the resolution of the HST is insufficient to study the base of the jets. Instead the *interaction* of the wind or jet with the surrounding medium must be used to constrain both the properties of the underlying wind and to establish connections between mass loss and accretion.

Strong evidence that jet power is linked to disk accretion in sources with optically-visible jets comes from the good correlation between the Hα and [OI] line luminosities and the infrared excess emission tracing the inner region of circumstellar disks (Cabrit et al. 1990). In deeply embedded systems, the correlation between the source bolometric luminosities (assumed to derive mainly from accretion in these objects) and outflow mechanical luminosities and momenta obtained from the high-velocity CO emission may provide further evidence that accretion and mass ejection are directly linked (Cabrit & Bertout 1992). Assuming momentum is conserved in the interaction between the driving wind and the ambient gas (which is the case if the shocks are highly radiative), then the total wind momentum, $M_{\rm w} V_{\rm w}$, must be equal to that observed in the swept-up molecular gas, $M_{\rm CO} V_{\rm CO}$. Observations of the molecular gas may therefore be used to estimate the mass-loss rate in the wind. Typical values for the mass and velocity of the CO flows are $M_{\rm CO} \sim 1.5$ $\rm M_\odot$, $V_{\rm CO} \sim 15$ km s^{-1}, and the outflows last for the full lifetime of the embedded protostellar phase, $\tau \sim 10^5$ yr. Assuming a driving wind speed of 200 km s^{-1}, the mass-loss rate in the wind is $\dot{M}_{\rm w} \sim (M_{\rm CO} V_{\rm CO})/(\tau V_{\rm w}) \sim 10^{-6}$ $\rm M_\odot$ yr^{-1}. The mean accretion rate needed to form a solar mass star during the embedded protostellar phase is $\dot{M}_{\rm acc} \sim 10^{-5}$ $\rm M_\odot$ yr^{-1}, implying $\dot{M}_{\rm w}$ is a fraction $f \sim 0.1$ times the accretion rate.

Measurements of the width of the optical jets HH30 and HH34 in HST images show they are resolved, with widths extrapolated back to the driving star of $0.2''$ (Ray et al. 1996; Burrows et al. 1996). If the jets maintain their narrow opening angles to the disk surface, they would intercept the disk at radii ~ 15–45 AU. However, the jet velocities observed imply that the jets originate at $r \lesssim 1$ AU, indicating that the initial opening angle of the jets are probably quite large ($\gtrsim 60°$), and that the flows must be re-collimated further from the star.

Most of the current models for jet/wind generation use MHD winds generated in a disk. The picture originally proposed by Blandford & Payne (1982) has a poloidal magnetic field threading much of the inner disk. Material is accelerated along the field lines by centrifugal forces. A wind may also be generated by strong gradients in the magnetic pressure close to the disk/star boundary layer (Uchida & Shibata 1984, 1985; Pringle 1989). The model described by Shu et al. (1988; 1994, and subsequent work) has the flow originating from a cusp through which the magnetic field lines pass, either at the interface between the disk and a protostar rotating at break-up, or at the inner radius of a disk where it intercepts the stellar magnetosphere. The value of $f = \dot{M}_{\rm w}/\dot{M}_{\rm acc} \sim 0.1$ can be reproduced by these models.

3.3. Flow variability

The wealth of structure observed in optical jets reveals both temporal and spatial variability. Multiple knots are interpreted as internal working surfaces, and exhibit optical line ratios indicative of shock velocities of 40–100 km s^{-1} (Mundt et al. 1987). Proper motion measurements and radial velocities show that the knots themselves are moving at velocities 200–300 km s^{-1}, and the separation of the knots suggest variability on timescales of ~ 10 yr. Bowshocks resulting from the interaction of the jet with the interstellar medium are separated on scales corresponding to 10^2–10^3 yr (e.g., Reipurth et al. 1997).

The large "S"-shaped optical jets show that the direction of the jets does not remain constant, wandering on timescales of 10^4 yr. Evidence that a wandering jet has also had a major influence on molecular outflow structure has been observed for the RNO43 flow in Orion (Bence et al. 1996). This flow is much older than HH211, and the jet has travelled several parsecs through the surrounding molecular cloud. Figure 7 displays the molecular line emission along with the location of Hα and $\rm H_2$ bowshocks in RNO43. The optical and infrared lines have cooling timescales of only a few years, while the CO cools on a timescale of

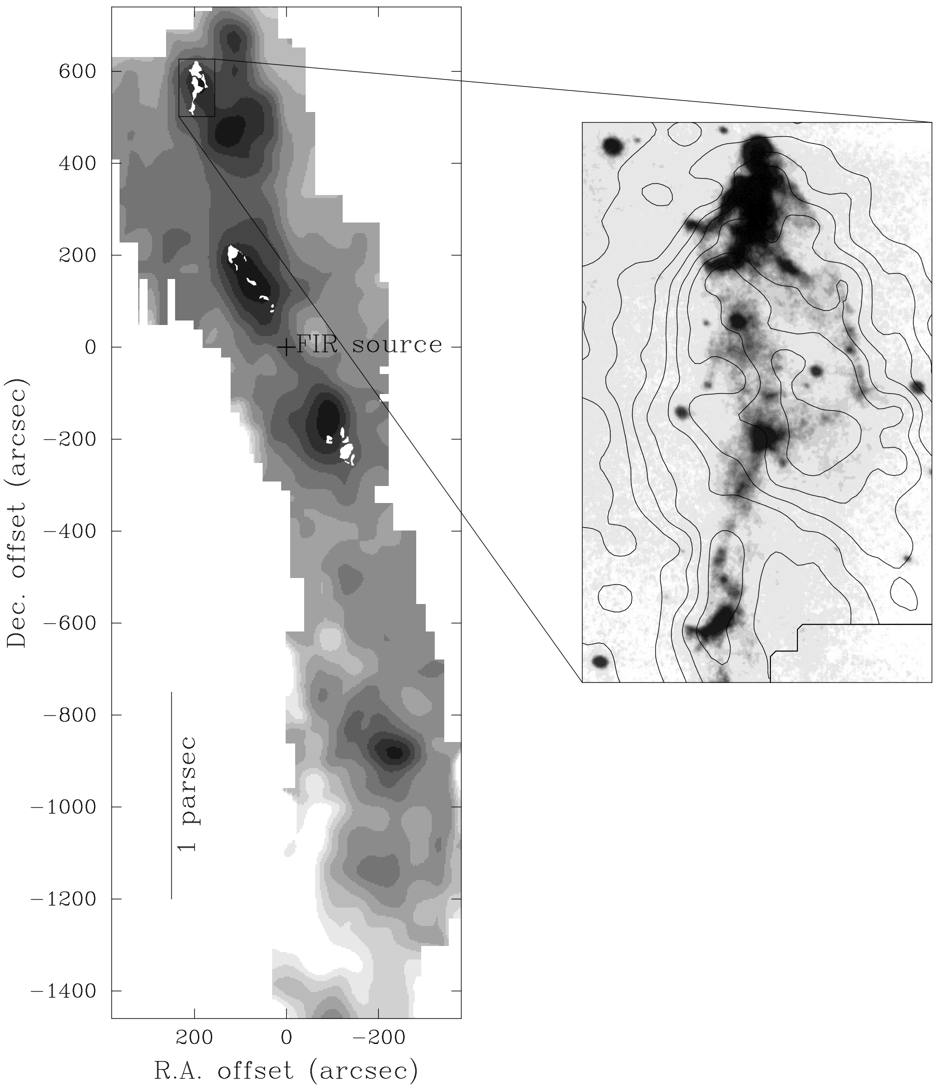

Figure 7. *Left:* greyscale of the CO J=2–1 emission from the RNO43 outflow (adapted from Bence et al. 1996). The locations of Hα emission are marked as white outlines. *Right:* the detailed correspondence between the CO(2–1) (contours) and the Hα emission (greyscale) illustrate that the molecular gas has been entrained by the bowshock and driving jet.

$\sim 10^3$ yr. The Hα emission therefore shows the location of a very recent passage of the jet through the molecular cloud. There is a clear correspondence between structures observed in the CO flow towards the north of RNO43 and the Hα bowshocks (Figure 7). The kinematics of the CO emission are also consistent with a bowshock, and suggest that the line profiles of the CO can be used elsewhere in the molecular flow to deduce the passage of the jet in the more distant past. The direction of the RNO43 jet appears to have been varying in time, carving out a cone with a full opening angle of $\sim 26°$.

Variations in the jet speed, jet direction, and mass-loss rate are needed to explain all the observed features of optical jets and molecular flows, implying an accretion history that is far from steady. MHD instabilities may be responsible for the spacing of the knows (e.g., Ouyed et al. 1997), and FU Orionis outbursts could explain the multiple bowshocks on larger scales. Jet wandering may be caused by the influence of a stellar companion or multiple system on the disk (Larwood & Papaloizou 1997), or by the accretion of material with anomalously high angular momentum.

3.4. Outflow evolution and the role of wide-angle winds

While optically-visible sources have common features of high-collimated jets and terminal bowshocks, a considerable variety of structures is observed for molecular outflows, from the highly-collimated molecular jets associated with deeply embedded protostars of which HH211 is an extreme example, to those with opening angles of 90° or more (e.g., B5-IRS1: Velusamy & Langer 1998). The wide-angle flows are typically associated with protostars visible in the optical or near-infrared, some of which also have optical jets aligned with the outflow symmetry axis. While jets are clearly important for driving the young flows and do an excellent job of explaining the CO bowshock structures observed in RNO43, it is less clear that the jets can explain the wide opening angles of the older flows. As Figures 5–7 demonstrate, the result of the passage of a jet through ambient gas is not the smooth, regular structures observed in optical and near-infrared reflection nebulae and molecular shells such as B5-IRS1.

The embedded protostars TMC1 and TMC1A in Taurus illustrate the conical outflow lobes often observed, traced by 1.6 μm reflection nebulosity and high-velocity molecular line emission (Figure 8). The infrared emission is associated with the blueshifted outflow lobe in each source, and has very well-defined and smooth edges tracing a cone with opening angle $\sim 45°$, extending to within a few 100 AU of the central protostar (Chandler et al. 1996). Recent near-infrared imaging of TMC1 using the HST now shows this structure extends smoothly to within 20 AU of the source, and has for the first time identified a jet lying along the symmetry axis (Hancock et al. 1998). It is unlikely that this cavity can have been carved out by the wandering of the jet, so we must now consider the possibility of a wide-angle wind component to explain these older sources (e.g., Shu et al. 1995; Ostriker 1997). This wind may contain only small fraction of the energy and momentum compared with the jet, but it may be extremely important for clearing away the remains of the envelope, to reveal the young star optically.

Besides an apparent evolution in the opening angle of molecular outflows there is also evidence that the outflow power declines with time (Bontemps et

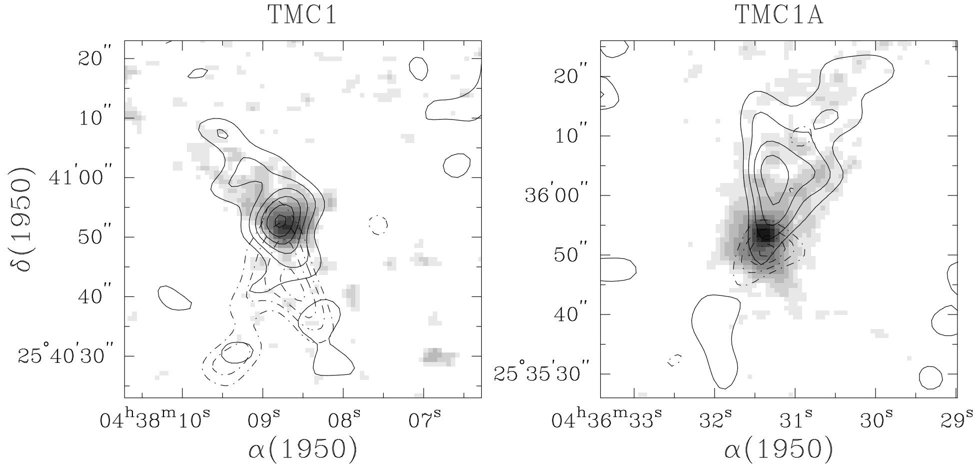

Figure 8. Contours of blueshifted (solid lines) and redshifted (dotted lines) CO J=1–0 emission from the protostars TMC1 and TMC1A, imaged using the Owens Valley millimetre interferometer, are overlaid on a greyscale of the 1.6-μm reflection nebulosity (Chandler et al. 1996). Both the high-velocity gas and the near-infrared emission trace conical outflow lobes with opening angles $\sim 45°$.

al. 1996): the momentum flux declines from that measured for the youngest objects ($\lesssim 10^4$ yr) by a factor of ~ 50 throughout the lifetime of the embedded phase, $\sim 10^5$ yr. This result suggests either that $\dot{M}_{\rm acc}$ decreases steadily with increasing age, or that f is not constant. These two alternatives cannot yet be distinguished.

4. Conclusions

In the last five years the angular resolution needed to resolve circumstellar disks has finally been achieved, and radial density profiles are even beginning to be measured. A close link between disk accretion and mass loss has been established, and the spectacular images of stellar jets obtained using the HST and wide-field imaging reveals structure on many size scales, suggesting that accretion is episodic. However, images still contain only a few resolution elements across the disks, and many of the disk properties must still be obtained through indirect methods such as modelling of spectral energy distributions. In particular, several important questions remain to be answered: what is the nature of the viscosity in circumstellar disks? How are winds and jets driven? How are jets collimated? Breakthroughs in these areas require an order of magnitude increase in the spatial resolution, and this will be achieved by the large millimetre arrays under development in the US and in Europe, and the Smithsonian Submillimeter Array. We thus anticipate that in the next ten years our understanding of accretion and mass loss in star formation will increase dramatically.

Acknowledgments. The authors thank Anne Dutrey, Jane Greaves, Wayne Holland, Dave Koerner, Leslie Looney, and Jeff Hester, for providing figures for this review. JSR acknowledges support from a Royal Society Fellowship, and CJC is funded by an Advanced Fellowship from the UK Particle Physics and Astronomy Research Council.

References

Adams, F. C., & Shu, F. H. 1986, ApJ, 308, 836

André, P., & Montmerle, T. 1994, ApJ, 420, 837

André, P., Ward-Thompson, D., & Barsony, M. 1993, ApJ, 406, 122

Bachiller, R. 1996, ARA&A, 34, 111

Backman, D. E., & Paresce, F. 1993, in Protostars and Planets III, ed. E. H. Levy & J. I. Lunine, University of Arizona Press, Tucson, 1253

Bally, J., Devine, D., & Alten, V. 1996, ApJ, 473, 921

Beckwith, S. V. W., Sargent, A. I., Chini, R. S., & Güsten, R. 1990, AJ, 99, 924

Bence, S. J., Richer, J. S., & Padman, R. 1996, MNRAS, 279, 866

Blandford, R. D., & Payne, D. G. 1982, MNRAS, 199, 883

Bodenheimer, P. 1995, ARA&A, 33, 199

Bontemps, S., André, P., Terebey, S., & Cabrit, S. 1996, A&A, 311, 858

Burrows, C. J., et al. 1995, BAAS, 27, 1329

Burrows, C. J., et al. 1996, ApJ, 473, 437

Cabrit, S., & Bertout, C. 1992, A&A, 261, 274

Cabrit, S., Edwards, S., Strom, S. E., & Strom, K. M. 1990, ApJ, 354, 687

Carr, J. S., & Tokunaga, A. T. 1992, ApJ, 393, L67

Carr, J. S., Tokunaga, A. T., Najita, J., Shu, F. H., & Glassgold, A. E. 1993, ApJ, 411, L37

Cernicharo, J., & Reipurth, B. 1996, ApJ, 460, L57

Chandler, C. J., & Richer, J. S. 1997, in Low Mass Star Formation – from Infall to Outflow: Poster proceedings of IAU Symposium No. 182 on Herbig-Haro Objects and the Birth of Low Mass Stars, ed. F. Malbet & A. Castets, 76

Chandler, C. J., Carlstrom, J. E., Scoville, N. Z., Dent, W. R. F., & Geballe, T. R. 1993, ApJ, 412, L71

Chandler, C. J., Carlstrom, J. E., & Scoville, N. Z. 1995, ApJ, 446, 793

Chandler, C. J., Terebey, S., Barsony, M., Moore, T. J. T., Gautier, T. N. 1996, ApJ, 471, 308

Close, L. M., Roddier, F., Northcott, M. J., Roddier, C., & Graves, J. E. 1997, ApJ, 478, 766

Devine, D., Bally, J., Reipurth, B., & Heathcote, S. 1997, AJ, 114, 2095

Dutkevitch, D. 1995, PhD Thesis, Univ. Massachusetts

Dutrey, A., Guilloteau, S., & Simon, M. 1994, A&A, 286, 149

Dutrey, A., Guilloteau, S., Duvert, G., Prato, L., Simon, M., Schuster, K., & Ménard, F. 1996, A&A, 309, 493

Eislöffel, J. 1997, IAU Symp. 182, Herbig-Haro Flows and the Birth of Low Mass Stars, ed. B. Reipurth & C. Bertout, Kluwer, Dordrecht, 93

Eislöffel, J., & Mundt, R. 1997, AJ, 114, 280

Gammie, C. F. 1996, ApJ, 457, 355

Greaves, J. S. et al. 1998, ApJ, in press

Guilloteau, S., Dutrey, A., & Gueth, F. 1997, IAU Symp. 182, Herbig-Haro Flows and the Birth of Low Mass Stars, ed. B. Reipurth & C. Bertout, Kluwer, Dordrecht, 365

Hancock, T., Terebey, S., Van Buren, D., Padgett, D. L., & Brundage, M. 1998, BAAS, 30, 828

Hartigan, P., Morse, J. A., & Raymond, J. 1994, ApJ, 436, 125

Henning, T., Pfau, W., Zinnecker, H., & Prusti, T. 1993, A&A, 276, 129

Holland, W. S., et al. 1998, Nature, 392, 788

Jayawardhana, R., Fisher, S., Hartmann, L., Telesco, C., Piña, R., & Fazio, G. 1998, ApJ, 503, L79

Jensen, E. L. N., Mathieu, R. D., & Fuller, G. A. 1994, ApJ, 429, L29

Jensen, E. L. N., Mathieu, R. D., & Fuller, G. A. 1996, ApJ, 458, 312

Jura, M. 1991, ApJ, 383, L79

Kalas, P., & Jewitt, D. 1995, AJ, 110, 794

Kitamura, Y., Kawabe, R., & Saito, M. 1996, ApJ, 465, L137

Koerner, D. W., Ressler, M. E., Werner, M. W., & Backman, D. E. 1998, ApJ, 503, L83

Lada, C. J. 1985, ARA&A, 23, 267

Larwood, J. D., & Papaloizou, J. C. B. 1997, MNRAS, 285, 288

Lay, O. P., Carlstrom, J. E., Hills, R. E., & Phillips, T. G. 1994, ApJ, 434, L75

Lay, O. P., Carlstrom, J. E., & Hills, R. E. 1995, ApJ, 452, L73

Lay, O. P., Carlstrom, J. E., & Hills, R. E. 1997, ApJ, 489, 917

Looney, L. W., Mundy, L. G., & Welch, W. J. 1997, ApJ, 484, L157

McCaughrean, M. J., & O'Dell, C. R. 1996, AJ, 111, 1977

McCaughrean, M. J., Rayner, J. T., & Zinnecker, H. 1994, ApJ, 436, L189

McCaughrean, M. J., et al. 1998, 492, L157

Mundt, R., Brugel, E. W., & Bührke, T. 1987, ApJ, 319, 275

Mundy, L. G., et al. 1996, ApJ, 464, L169

Najita, J., Carr, J. S., Glassgold, A. E., Shu, F. H., & Tokunaga, A. T. 1996, ApJ, 462, 919

Nakamoto, T., & Nakagawa, Y. 1995, ApJ, 445, 330

Natta, A. 1993, ApJ, 412, 761

Osterloh, M., & Beckwith, S. V. W. 1995, ApJ, 439, 288

Ostriker, E. C. 1997, ApJ, 486, 291

Ouyed, R., Pudritz, R. E., & Stone, J. M. 1997, Nature, 385, 409

Padman, R., Bence, S., & Richer, J. 1997, IAU Symp. 182, Herbig-Haro Flows and the Birth of Low Mass Stars, ed. B. Reipurth & C. Bertout, Kluwer, Dordrecht, 123

Pringle, J. E. 1981, ARA&A, 19, 137

Pringle, J. E. 1989, MNRAS, 236, 107

Pudritz, R. E., Wilson, C. D., Carlstrom, J. E., Lay, O. P., Hills, R. E., & Ward-Thompson, D. 1996, ApJ, 470, L123

Ray, T. P., Mundt, R., Dyson, J. E., Falle, S. A. E. G., & Raga, A. C. 1996, ApJ, 468, L103

Reipurth, B., & Heathcote, S. 1997, IAU Symp. 182, Herbig-Haro Flows and the Birth of Low Mass Stars, ed. B. Reipurth & C. Bertout, Kluwer, Dordrecht, 3

Reipurth, B., Bally, J., & Devine, D. 1997, AJ, 114, 2708

Richer, J. S., Hills, R. E., & Padman, R. 1992, MNRAS, 254, 525

Roddier, C., Roddier, F., Northcott, M. J., Graves, J. E., & Jim, K. 1996, ApJ, 463, 326

Saigo, K., & Hanawa, T. 1998, ApJ, 493, 342

Shakura, N. I., & Sunyaev, R. A. 1973, A&A, 24, 337

Shu, F. H., Lizano, S., Ruden, S. P., & Najita, J. 1988, ApJ, 328, L19

Shu, F., Najita, J., Ostriker, E., Wilkin, F., Ruden, S., & Lizano, S. 1994, ApJ, 429, 781

Shu, F. H., Najita, J., Ostriker, E. C., & Shang, H. 1995, ApJ, 455, L155

Skrutskie, M. F., Dutkevitch, D., Strom, S., E., Edwards, S., Strom, K. M., & Shure, M. A. 1990, AJ, 99, 1187

Smith, B. A., & Terrile, R. J. 1984, Science, 226, 1421

Stahler, S. W., Korycansky, D. G., Brothers, M. J., & Touma, J. 1994, ApJ, 431, 341

Uchida, Y., & Shibata, K. 1984, PASJ, 36, 105

Uchida, Y., & Shibata, K. 1985, PASJ, 37, 515

Velusamy, T., & Langer, W. D. 1998, Nature, 392, 685